

A NOVEL DOUBLE-WINDING PERMANENT MAGNET FLUX MODULATED MACHINE FOR STAND-ALONE WIND POWER GENERATION

Linni Jian^{1, 2}, Jianing Liang^{1, 2, *}, Yujun Shi^{1, 2}, and G. Xu^{2, 3}

¹Shenzhen Institutes of Advanced Technology, Chinese Academy of Sciences, Shenzhen 518055, China

²The Chinese University of Hong Kong, Sha Tin, Hong Kong SAR, China

³Department of Electrical Engineering, Tongji University, Shanghai 200092, China

Abstract—This paper proposes a novel double-winding flux modulated permanent magnet machine (FMPM) for stand-alone wind power generation. Based on the flux-modulating effect, a concentrated winding set and a distributed winding set can be artfully equipped on one stator component. This makes the proposed machine possessing much simpler structure than traditional double-winding double-stator PM machines. Comparative study shows that the proposed FMPM can offer higher torque capability and stronger flux adjustability than the existing single-winding FMPMs.

1. INTRODUCTION

Up till now, there are still more than 2 billion people living in remote areas having no electrical grid connection. Nevertheless, developing electrical grids in these areas is not a proper solution considering economy. Therefore, stand-alone wind power generation which is able to be used in off-grid systems has attracted increasing attention [1]. One of its key technologies lies in the high performance small-to-medium wind power generator. Generally, such generators are expected to satisfy the following requirements:

Received 23 July 2013, Accepted 22 August 2013, Scheduled 5 September 2013

* Corresponding author: Jianing Liang (jn.liang@siat.ac.cn).

1) Stand-alone wind power generators should be with light weight and compact size, so that they are readily for installation on tower pole;

2) Stand-alone wind power generators should be able to offer low-speed direct-drive operation, so as to get rid of the mechanical gearbox;

3) Stand-alone wind power generators should be with high efficiency for energy conversion.

Hence, multiple-pole PM machine which can offer high power density and low power losses becomes a competitive candidate [2, 3]. However, due to the weak flux adjustability, traditional PM generators usually produce a highly fluctuating output voltage under varying wind speeds. This will arouse much trouble for the design of power electronic converters. Recently, lots of efforts have been made on solving this problem. In [4], a double-stator PM generator with cup-rotor was proposed. By online adjusting the connection of the two sets of windings, the fluctuation of the output voltage can be confined within an acceptable scale. Nevertheless, this machine suffers from its complicated mechanical structure, and the adjustment of winding connection will increase additional hardware circuits which may reduce the robustness of the whole system. In [5], a hybrid PM machine was proposed. A DC winding is engaged to adjust the flux density in air-gap, so as to keep the output voltage stable under varying wind speeds. However, it needs a separate controllable DC power source which will inevitably increase the overall cost of the system.

The purpose of this paper is to propose a novel type of PM machine for stand-alone wind power generation. Firstly, its working principle is based on the flux-modulation effect [6–9]. The prominent difference between conventional PM machine and flux-modulated PM machine is that the former relies on the fundamental field component to achieve energy conversion and transmission, while the latter relies on the field harmonics to do so. It has been proven that PM flux modulated machine can offer higher torque density and better ventilation than traditional PM machines [10]. Secondly, it adopts double-winding, so that it can offer even higher power density and stronger flux-weakening capability. In Section 2, the configuration of the proposed machine is introduced. Its operating principle analysis based on finite element method (FEM) is elaborated in Section 3. Section 4 is devoted to the comparative investigation among the potential alternatives. Finally, conclusions are drawn in Section 5.

2. CONFIGURATION OF THE PROPOSED MACHINE

2.1. Machine Structure

Figure 1(a) shows the configuration of a traditional stand-alone wind-power generation system in remote areas. It consists of a wind turbine to capture wind energy and convert it into mechanical power, a wind power generator to convert mechanical power into electrical power, a three-phase bridge rectifier to perform simple AC-DC conversion, a DC-DC converter to regulate the rectified DC voltage, and a battery pack for energy storage. For AC loads, an inverter is used to perform DC-AC conversion, while for DC loads, a DC-DC converter is engaged to regulate the voltage level.

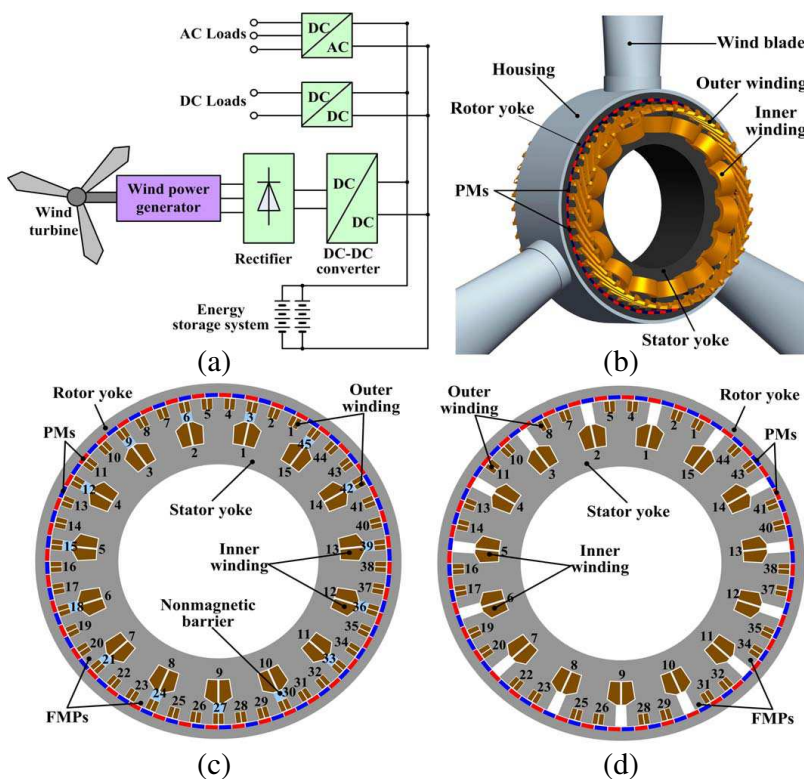


Figure 1. (a) Stand-alone wind power system. (b) Configuration of proposed machine. (c) Cross section view-case 1: with fully filled outer winding. (d) Cross section view-case 2: with partially filled outer windings.

Figure 1(b) shows the constitution of the proposed generator. It adopts outer-rotor topology, and the wind blades are directly installed on the outer rotor in order to get rid of the transmission mechanisms. 40-pole-pair PMs are mounted on the inside surface of the outer rotor. Two sets of armature windings are equipped in the stator: the inner windings are concentrated windings, which are deployed in the 15 inner air-slots; the outer windings are distributed windings, which are deployed among the flux-modulated air-slots (FMAs) located adjacent to the flux-modulating poles (FMPs). In Fig. 1(c), the nonmagnetic barriers are employed, so that the outer windings are fully filled in all the 45 FMAs. While in Fig. 1(d), the nonmagnetic barriers do not exist, and the outer windings are partially filled in these 30 FMAs. The pole-pair numbers of inner windings and outer windings are both equal to 5.

2.2. Winding Connection

As illustrated in Figs. 1(c) and (d), double layer conductors are adopted in both the inner and outer windings. Fig. 2(a) illustrates the slot electric vecogram in the inner windings. Since the pole-pair number of inner windings is designed as 5, the electrical angle between the adjacent two slot equals 120 Degrees. Thus, the concentrated winding connection as shown in Fig. 3(a) can be adopted. Fig. 2(b) illustrates the slot electric vecogram in the outer windings for Case 1, in which the nonmagnetic barriers are employed, and all the 45 FMAs are occupied. The pole-pair number and pole pitch equal 5 and 4 slots, respectively, so that the electrical angle spanned by a winding coil

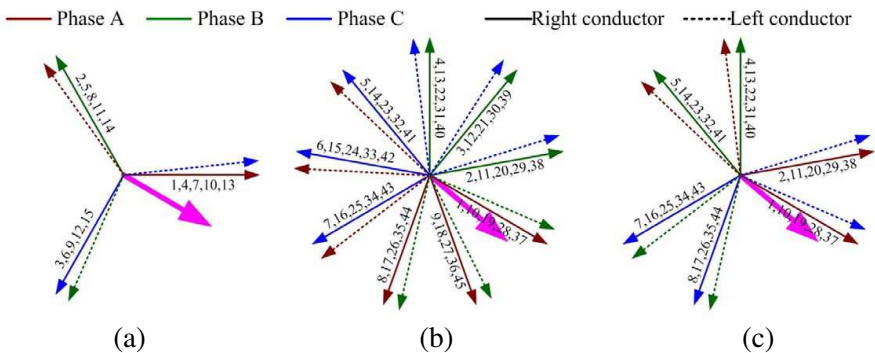


Figure 2. Slot electric vectogram in winding connections. (a) Inner winding. (b) Outer winding-case 1. (c) Outer winding-case 2.

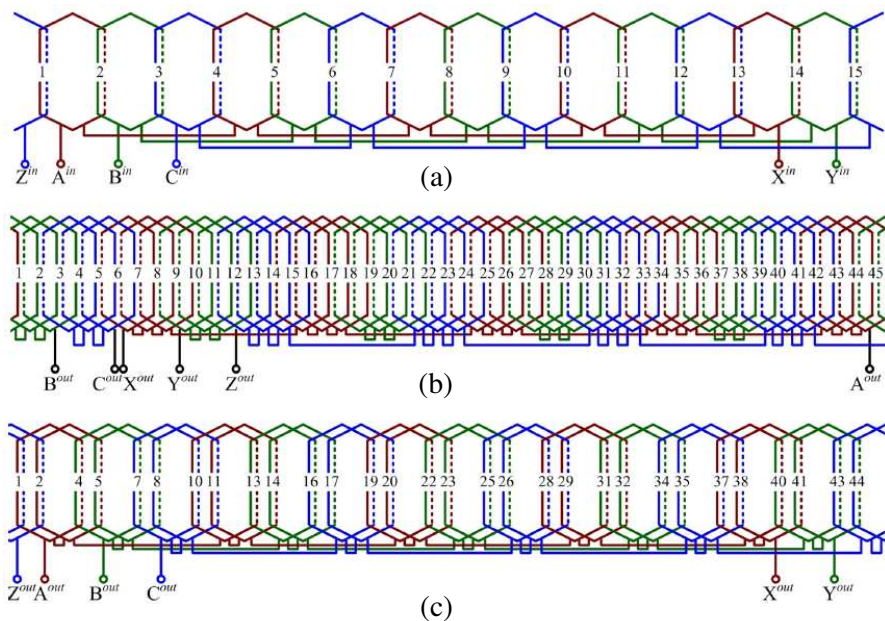


Figure 3. Winding connections. (a) Inner winding. (b) Outer winding-case 1. (c) Outer winding-case 2.

equals 160 Degrees. The corresponding winding connection is shown in Fig. 3(b). Fig. 2(c) illustrates the slot electric vecogram in the outer windings for Case 2, in which the nonmagnetic barriers do not exist, and only 30 FMAs are occupied. The pole pitch equals 3 slots, and the electrical angle spanned by a winding coil equals 120 Degrees. The corresponding winding connection is shown in Fig. 3(c).

The connections of the inner and outer windings are shown in Fig. 4. For the same phase, such as Phase A, there is no phase angle difference between the inner and outer winding as illustrated in the vector diagram in Fig. 4. Such a connection mode can ensure the maximum electromechanical energy conversion capability. In the machine presented in [4], there are 6 connection modes between its two sets of windings, which is achieved by a sophisticated matrix converter. By online changing the connection modes, the output voltage can be controlled. However, the adoption of matrix converter will definitely increase the cost and also reduce the robustness of the whole system. In our proposed machine, the connection mode of the two sets of windings does not need to change, and the output voltage is controllable by flux-weakening operation which will be discussed later.

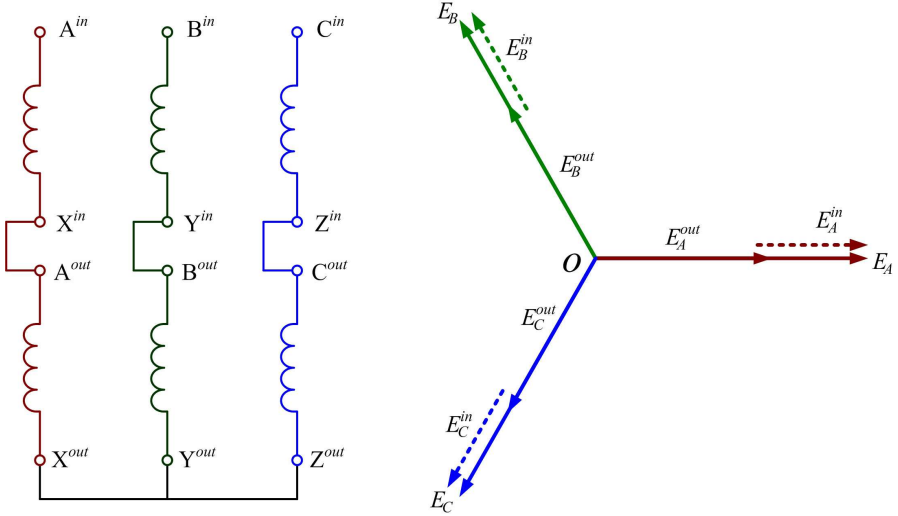


Figure 4. Connection of two sets of windings and vector diagrams.

3. OPERATING PRINCIPLE ANALYSIS

In traditional PM machines, the pole-pair numbers (PPN) of armature windings is designed the same as the PPN of PMs, so that the electromechanical energy conversion can be achieved through the interaction of fundamental components of the magnetic fields. Nevertheless, the PPN of the armature windings is no longer equal to that of the PM poles in flux modulated PM machines. The operating principle of flux modulated PM machines relies on the flux modulating effect, also termed as magnetic-gearing effect [11, 12], arising from the non-even magnetic field path caused by the FMPs. Assume that p_r and p_w denote the PPN of PMs on the rotor and the PPN of armature windings, respectively and that N_s denotes the number of FMPs installed on the stator. After modulation, the magnetic field in the airgap is compounded by a series of harmonic components. The PPNs of the harmonic component $H_r(i, j)$ excited by the rotor PMs can be determined by:

$$p(i, j) = |ip_r + jN_s| \quad (1)$$

where $i = 1, 2, 3, \dots, \infty$ and $j = 0, \pm 1, \pm 2, \pm 3, \dots, \pm\infty$, and the corresponding rotational speed can be given by:

$$\omega(i, j) = \frac{ip_r}{ip_r + jN_s} \omega_r \quad (2)$$

where ω_r is the rotational speed of the rotor.

Similarly, the PPNs of the harmonic component $H_w(i, j)$ excited by the armature windings can be determined by:

$$p'(i, j) = |ip_w + jN_s| \quad (3)$$

and the corresponding rotational speed is given by:

$$\omega'(i, j) = \frac{ip_w}{ip_w + jN_s} \omega_s \quad (4)$$

where ω_s is the rotational speed of the electromagnetic flux vector.

As long as the following relationships are satisfied:

$$N_s = p_r + p_w \quad (5)$$

$$\omega_s = -\frac{p_r}{p_w} \omega_r \quad (6)$$

All the Equations (1)–(6) consist of the essence of the theory of magnetic modulating effect which can be found in details in [13]. It can be known from (1)–(6) that the harmonic component $H_r(1, -1)$ excited by the rotor PMs and the harmonic component $H_w(1, 0)$ excited by the armature windings have the same PPN (PPN = 5) and the same rotational speed. Thus, stable electromechanical energy conversion can be achieved by the interaction of harmonics $H_r(1, -1)$ and $H_w(1, 0)$. Moreover, the harmonic component $H_r(1, 0)$ excited by the rotor PMs and the harmonic component $H_w(1, -1)$ excited by the armature windings also have contribution to the stable electromechanical energy conversion, since they have the same PPN (PPN = 40) and the same rotational speed as well.

Finite element method (FEM) has been extensively used to analyze the performance of electromechanical devices [14–16]. Herein, it is also employed to demonstrate the operating principle of the proposed machine. Fig. 5 shows the flux distribution excited by the PMs obtained from Ansoft, which is a widely employed software for electromagnetic design and analysis. It can be observed that the harmonic component $H_r(1, -1)$ (with PPN = 5) goes through the two windings simultaneously. In addition, the excited flux density distribution along the circumferences that go through the central points of the inner and outer slot areas, respectively, are illustrated in Figs. 6 and 7. Their space harmonic spectra shows that the amplitudes of the harmonic component $H_r(1, -1)$ equal 0.068 T and 0.059 T in the inner and outer slot areas. This proves that the magnetic field excited by the PMs on the rotor can effectively couple with both the inner windings (concentrated windings) and outer windings (distributed windings) due to the flux-modulation effect. It is worth noting that the fundamental component of the magnetic field excited by the PMs is short-circuited by the iron yokes on the stator and does

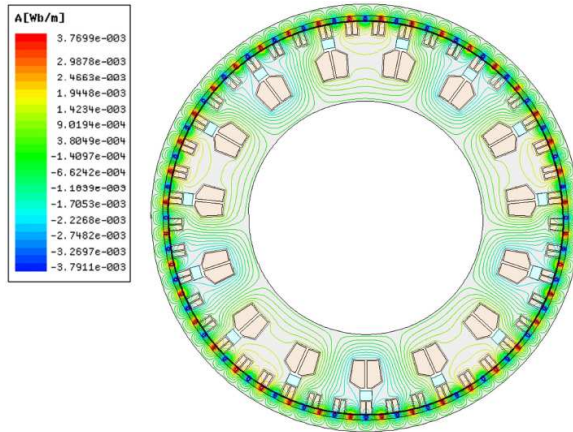


Figure 5. Flux distribution at no-load.

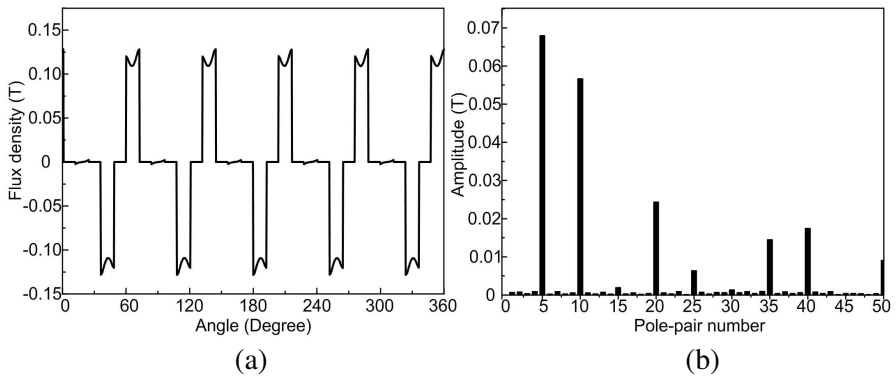


Figure 6. Flux density distribution in inner slots excited by PMs. (a) Flux density waveform. (b) Harmonic spectra.

not go through the inner windings, which is the reason that two stators have to be employed when designing double winding conventional PM machines which work with fundamental components [4].

The magnetic field produced by the windings is also assessed by using FEM. First, the PMs on the outer rotor are removed. Second, three-phase sinusoidal AC currents with the maximum current density $J = 3 \text{ A/mm}^2$ are injected into the inner windings. The calculated flux density distribution in the air-gap is shown in Fig. 8. It can be observed that the modulated harmonic component $H_w(1, -1)$ can be obtained to achieve electromagnetic coupling with the fundamental

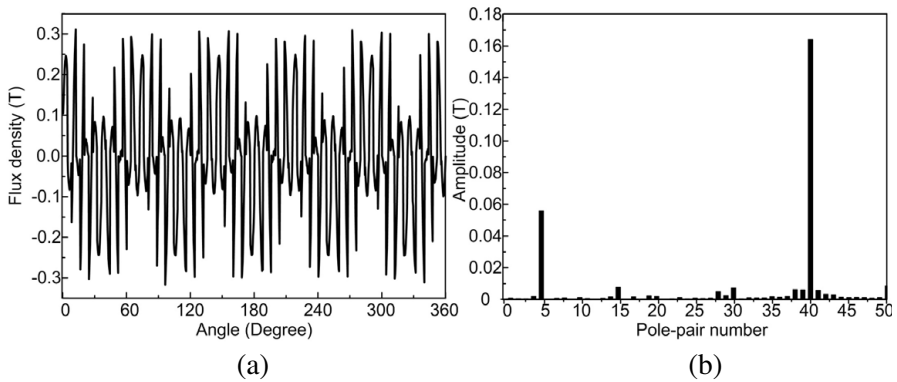


Figure 7. Flux density distribution in outer slots excited by PMs. (a) Flux density waveform. (b) Harmonic spectra.

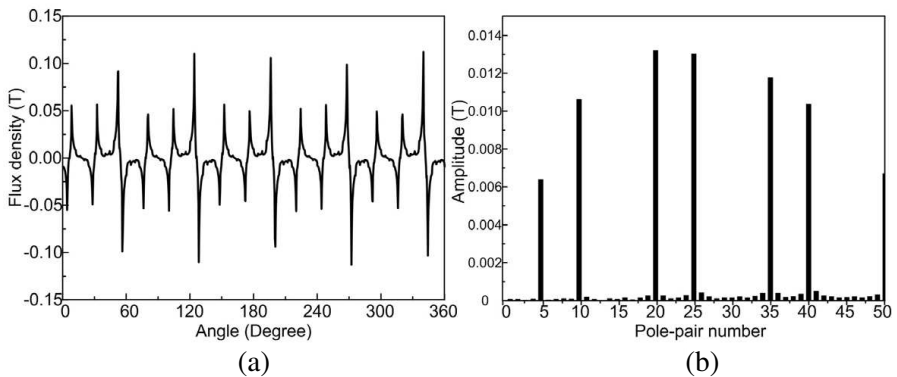


Figure 8. Flux density distribution in air-gap excited by inner windings.

component of the magnetic field produced by the PMs. Similarly, the flux distributions in the air-gap produced by the outer windings are given in Figs. 9 and 10, in which Fig. 9 shows Case 1 and the other Case 2.

In addition, assuming that the number of conductors in each slot equals 1, Fig. 11 gives the calculated back EMF waveforms (Phase-A) when rotor rotating at 150 rpm, which demonstrated that electric power can be generated by the electromagnetic coupling between the PMs and both windings.

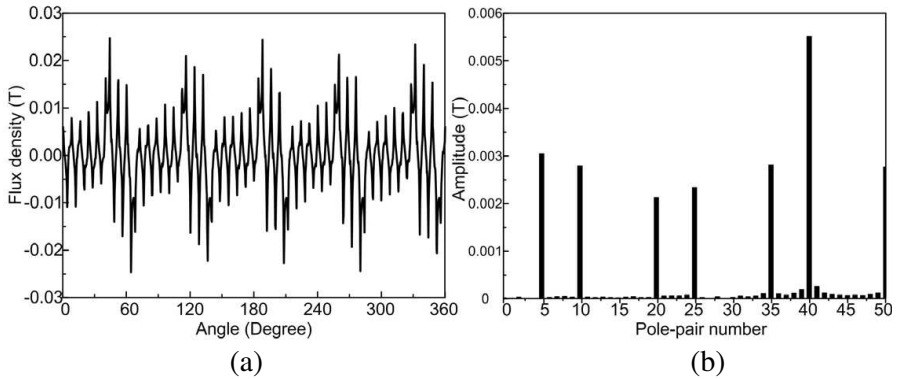


Figure 9. Flux density distribution in air-gap excited by outer windings-case 1. (a) Flux density waveform. (b) Harmonic spectra.

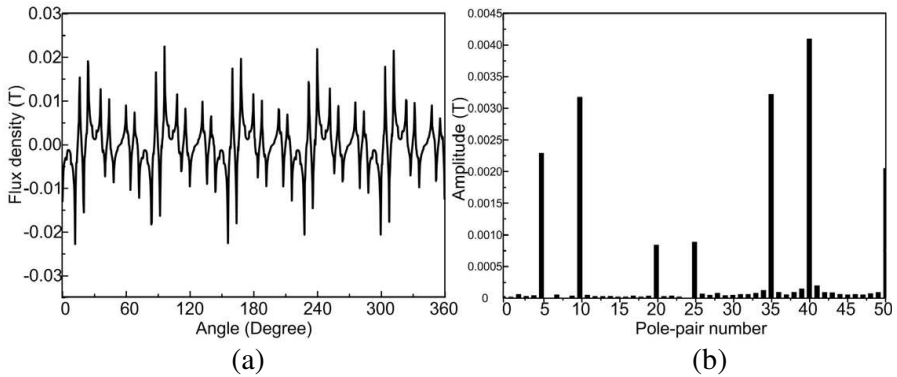


Figure 10. Flux density distribution in air-gap excited by outer windings-case 2. (a) Flux density waveform. (b) Harmonic spectra.

4. COMPARATIVE INVESTIGATION

In order to demonstrate the merits of the proposed double-winding PM flux-modulated machines (PMFMs), two types of existing single-winding PMFMs as shown in Fig. 12 are selected for comparative investigation. Case 3 has concentrated windings as presented in [8], and Case 4 is equipped with distributed windings as presented in [17]. For fair comparison, the rotor topologies of these four machines are exactly the same. In addition, the stator iron yoke of Case 3 is identical to that of Cases 1 and 2, and the dimensions of the FMPs and FMAs on Case 4 are the same as that on Cases 1–3. Some identical design data are listed in Table 1.

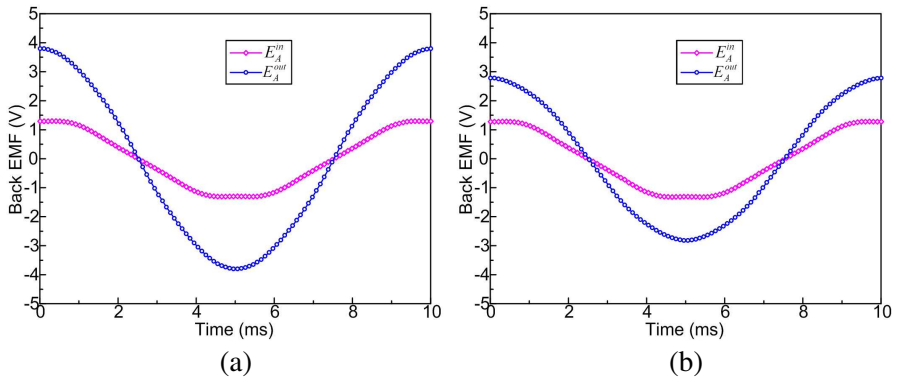


Figure 11. Back EMF waveforms. (a) Case 1. (b) Case 2.

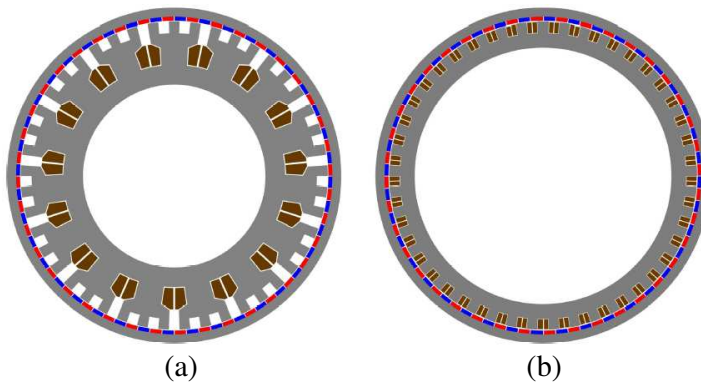
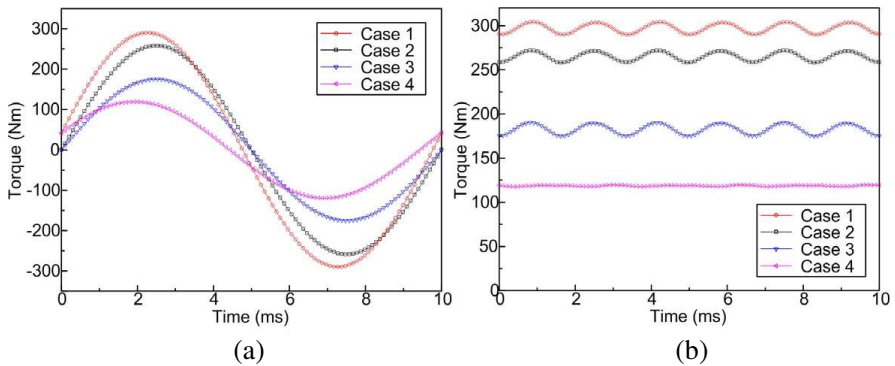


Figure 12. Existing single winding PMFMs for comparison. (a) Case 3: with concentrated windings. (b) Case 4: with distributed windings.

Time stepping finite element method (TSFEM) is used to conduct quantitative study. By locking the rotors and injecting ac currents to the armature windings, the torque capability can be obtained as shown in Fig. 13(a). Herein, the current density and frequency are set as 3.0 A/mm^2 and 100 Hz for all four cases. It can be observed that the double-winding machines exhibit much better torque capability than their single-winding counterparts. The maximum pull-out torques are equal to 296.3 Nm , 271.1 Nm , 182.9 Nm and 118.6 Nm for Cases 1, 2, 3 and 4, respectively. Thus, the torque capability of the proposed double-winding machines 1, 2 can offer improvements by 62.0% , 48.2%

Table 1. Identical design data for comparative study.

Outside radius of rotor	185 mm
Length of air-gap	0.8 mm
Outside radius of stator	162.2 mm
Axial length	110 mm
Thickness of PMs	4.2 mm
Pole arc coefficient	0.9
Remanence of PMs	1.23 T
Base speed	150 rpm

**Figure 13.** Comparison of torque characteristics. (a) Torque capability. (b) Torque ripples.

compared with the existing single winding machine 3, and by 149.8%, 128.6% compared with the existing machine 4. Fig. 13(b) gives the torque-time waveforms when keeping the rotors rotating at 150 rpm, which is the synchronous speed corresponding to the 50 Hz currents. It is demonstrated that the torque ripples are mainly caused by the concentrated windings.

All the four machines are designed with base speed equal to 150 rpm, and the limit for their back EMF (peak value) is set as 650 V. In traditional PM wind power generators, due to the very weak flux adjustability, the magnitude of back EMF goes up rapidly with increasing rotational speed of wind turbine. Thus, in order to protect

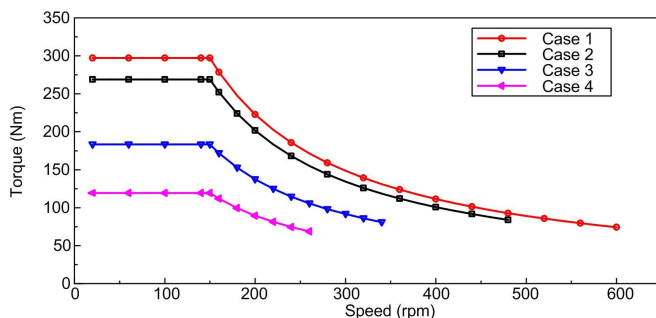


Figure 14. Comparison of torque-speed envelopes.

the power converters, generators have to be disconnected at strong winds. In the proposed double-winding FMPMs, the flux weakening capability can be significantly improved since the armature field is strengthened by engaging much more coils. Fig. 14 illustrates the calculated torque-speed envelopes of these four machines. It can be observed that the upper bound of speed range for constant-power generation is as high as 600 rpm in Case 1, which is 4 times of the base speed, while those in single-winding machine 3 and 4 are only 350 rpm and 275 rpm, respectively.

5. CONCLUSIONS

In this paper, a novel double-winding FMPM is proposed and analyzed. Based on the flux-modulating effect, a concentrated winding set and a distributed winding set can be artfully equipped on one stator component. This makes the proposed machine possessing much simpler structure than traditional double-winding double-stator PM machines. Comparative study demonstrates that the proposed FMPM can offer higher torque capability and stronger flux adjustability than the existing single-winding FMPMs.

ACKNOWLEDGMENT

This work was supported by a grant (Project 51107141) from the National Natural Science Foundation of China, and a research grant (JCY201110108) from the Science and Technology Innovation Committee of Shenzhen, China.

REFERENCES

1. Valenciaga, F. and P. Puleston, "High-order sliding control for a wind energy conversion system based on a permanent magnet synchronous generator," *IEEE Trans. on Energy Conversion*, Vol. 23, No. 3, 860–867, 2008.
2. Chen, J., C. Nayar, and L. Xu, "Design and finite-element analysis of an outer-rotor permanent-magnet generator for directly coupled wind turbines," *IEEE Trans. on Magn.*, Vol. 36, No. 5, 3802–3809, 2000.
3. Misron, N. B., S. Rizuan, R. N. Firdaus, C. Aravind Vaithilingam, H. Wakiwaka, and M. Nirei, "Comparative evaluation on power-speed density of portable permanent magnet generators for agricultural application," *Progress In Electromagnetics Research*, Vol. 129, 345–363, 2012.
4. Niu, S., K. Chau, J. Jiang, and C. Liu, "Design and control of a new double-stator cup-rotor permanent-magnet machine for wind power generation," *IEEE Trans. on Magn.*, Vol. 43, No. 6, 2501–2503, 2007.
5. Liu, C., K. Chau, J. Jiang, and L. Jian, "Design of a new outer-rotor permanent magnet hybrid machine for wind power generation," *IEEE Trans. on Magn.*, Vol. 44, No. 6, 1494–1497, 2008.
6. Xu, G., L. Jian, W. Gong, and W. Zhao, "Quantitative comparison of flux-modulated interior permanent magnet machines with distributed windings and concentrated windings," *Progress In Electromagnetics Research*, Vol. 129, 109–123, 2012.
7. Jian, L., G. Xu, J. Song, H. Xue, D. Zhao, and J. Liang, "Optimum design for improving modulating-effect of coaxial magnetic gear using response surface methodology and genetic algorithm," *Progress In Electromagnetics Research*, Vol. 116, 297–312, 2011.
8. Li, J., K. T. Chau, J. Jiang, C. Liu, and W. Li, "A new efficient permanent-magnet vernier machine for wind power generation," *IEEE Trans. on Magn.*, Vol. 46, No. 6, 1475–1478, 2010.
9. Liu, C. and K.-T. Chau, "Electromagnetic design and analysis of double-rotor flux-modulated permanent-magnet machines," *Progress In Electromagnetics Research*, Vol. 131, 81–97, 2012.
10. Fu, W. and S. Ho, "A quantitative comparative analysis of a novel flux-modulated permanent-magnet motor for low-speed drive," *IEEE Trans. on Magn.*, Vol. 46, No. 1, 127–134, 2010.

11. Li, X., K.-T. Chau, M. Cheng, and W. Hua, "Comparison of magnetic-gear permanent-magnet machines," *Progress In Electromagnetics Research*, Vol. 133, 177–198, 2013.
12. Jian, L., G. Xu, Y. Gong, J. Song, J. Liang, and M. Chang, "Electromagnetic design and analysis of a novel magnetic-gear-integrated wind power generator using time-stepping finite element method," *Progress In Electromagnetics Research*, Vol. 113, 351–367, 2011.
13. Jian, L. and K. Chau, "A coaxial magnetic gear with halbach permanent magnet arrays," *IEEE Trans. on Energy Conversion*, Vol. 25, No. 2, 319–328, 2010.
14. Zhao, W., M. Cheng, R. Cao, and J. Ji, "Experimental comparison of remedial single-channel operations for redundant flux-switching permanent-magnet motor drive," *Progress In Electromagnetics Research*, Vol. 123, 189–204, 2012.
15. Mahmoudi, A., S. Kahourzade, N. A. Rahim, and H. W. Ping, "Improvement to performance of solid-rotor-ringed line-start axial-flux permanent-magnet motor," *Progress In Electromagnetics Research*, Vol. 124, 383–404, 2012.
16. Lecointe, J.-P., B. Cassoret, and J.-F. Brudny, "Distinction of toothing and saturation effects on magnetic noise of induction motors," *Progress In Electromagnetics Research*, Vol. 112, 125–137, 2011.
17. Toba, A. and T. Lipo, "Generic torque-maximizing design methodology of surface permanent-magnet vernier machine," *IEEE Trans. on Ind. Appl.*, Vol. 36, No. 6, 1539–1546, 2000.